Catalysis Today 141 (2009) 195–204

Contents lists available at ScienceDirect

Catalysis Today

journal homepage: www.elsevier.com/locate/cattod

Structural changes of FCC catalyst from fresh to regeneration stages and associated coke in a FCC refining unit: A multinuclear solid state NMR approach

Babita Behera, Siddharth S. Ray *

Indian Institute of Petroleum, Dehradun 248005, India

ARTICLE INFO

Article history:
Available online 15 May 2008

Keywords:
FCC catalyst
Coke
Multinuclear solid state NMR

ABSTRACT

The changes in zeolitic structure (Y zeolite) of fresh, equilibrium, spent and regenerated FCC catalysts obtained from an Indian FCC refining unit were investigated by ^{29}Si magic angle spinning (MAS) and cross polarization (CP)-MAS, ^{27}Al MAS and multiple quantum MAS (MQMAS) NMR. Deconvoluted ^{29}Si MAS NMR along with ^{29}Si CP-MAS NMR of these four catalysts provide the detailed local structural changes occurring at all Si(*n*Al) sites. ^{27}Al MAS NMR provides the relative changes of tetrahedral (T_d) and octahedral (O_h) aluminum sites of the FCC catalysts at different stages of the cracker. Second order quadrupolar effect (SOQE) and quadrupole coupling constant (C_Q) obtained from both computation of ^{27}Al MQMAS and simulation of ^{27}Al 1D MAS spectra of these catalysts give imposition of structural asymmetries in T_d and O_h sites that can be correlated with catalytic activities. Local structural changes are explained by NMR and are supplemented by Si/Al ratio, shrinkage in unit cell size and crystallinity obtained from XRD and BET. Si(3Al) sites of Y zeolite are found to be more deactivated and may be the primary sites of coking. ^{13}C single hard pulse excitation (SHPE)-MAS, CP-MAS, cross polarization-dipolar dephasing (CPDD) NMR and CP dynamics analysis of hard coke extracted from the spent catalyst from the FCC unit reveal essential structural properties and nature of coke.

1. Introduction

Fluid catalytic cracking (FCC) is the most important and complicated process in petroleum refining, which is the most widely used refining process in the world to convert heavy petroleum fractions into gasolines, light olefins and cycle oils [1–4]. Forty-five percent of all the gasolines are produced from FCC worldwide. Solid catalysts are used in FCC process to achieve desirable selectivity and rate of product formation. In order to understand the function of such catalysts and to optimize their performances, it is necessary (a) to characterize the structure of catalytic materials and their surfaces, (b) to understand the interaction between reactant molecules and catalysts and (c) the mechanism of chemical reaction during the course of catalytic processes. FCC has assumed special importance in Indian context in the view of increasing demand for middle distillates and all the refineries have FCC units. Therefore, optimization with respect to Indian feedstocks, catalysts and product demand pattern is of great relevance. In India, the consumption of crude oils (in terms of refinery throughput) and petroleum products are 127.12 MMT and 111.56 MMT while the production of crude oil and petroleum product are 37.98 MMT and 118.23 MMT, respectively [5]. With such increasing demand, the country needs better technologies with crude and product optimization. Besides this, the coke on the catalysts greatly affects the unit's economy. Thus, for better understanding the chemistry of the FCC process we should have deep knowledge of nature and composition of feeds, structure of catalysts and nature of coke. This understanding helps in optimizing the process parameters of the reactor for a desired product slate.

Since FCC catalysts are solid acids composed of predominantly silica and alumina, the application of ^{27}Al, ^{29}Si and ^{1}H NMR provides a large number of information about the structure and acidity of the cracking catalysts [6,7]. The acidic (Brönsted) properties of these materials result from tetrahedral aluminum atoms connected through oxygen bridges to four silicon atoms. In this case the aluminum has a formal −ve charge balanced by +vely charged protons (acidic zeolites) or cations located on or near one of the bridging oxygen atom. Lewis acid sites are the electron deficient aluminum sites formed in some cases by dehydroxylation of every two Brönsted acid sites at higher temperatures. The catalytic cracking is generally carried out with Brönsted acid sites, sometimes, depending upon the reaction, Lewis sites are also involved. Modified Y zeolite (H-Y, USY, RE-Y) is the major

* Corresponding author at: Analytical Sciences Division, Indian Institute of Petroleum, Dehradun 248005, India. Tel.: +91 135 2660116 271; fax: +91 135 2660202.
E-mail addresses: ssray@iip.res.in, ssiddharthray@yahoo.com (S.S. Ray).

0920-5861/$ – see front matter © 2008 Elsevier B.V. All rights reserved.
doi:10.1016/j.cattod.2008.03.017

constituent of FCC catalysts contributing to cracking activity. It is postulated that the number of framework aluminum atoms and zeolitic unit cell size control both density and acid strength. In gas oil cracking, USY has fewer but stronger acidic sites than REY [4]. This is because the de-alumination process used to ultra stabilize USY removes many of the framework aluminum sites leaving only a fraction of the original cationic sites existing in Y sieves. Thus, for cracking aromatic feeds the USY may lose its advantage over REY due to more coke formation.

Progressive advancement in methodologies for both liquids and solids has made NMR a versatile tool for characterizing complex petroleum fractions, catalysts and coke [8]. ^{29}Si MAS NMR has been used to quantify the occurrence of silicon with zero, one, two, three and four aluminum neighbours and to indirectly infer the degree of isolation of aluminum sites. In most zeolites, up to Si/Al ratio of about 10, the strength of acid sites is inversely proportional to the concentration of framework aluminum. Above 10 the aluminum distribution does not significantly affect the acid strength. Modified Y zeolites generally contains five characteristic silicon peaks in NMR corresponding to Si(0Al), Si(1Al), Si(2Al), Si(3Al) and Si(4Al) sites with chemical shift ranges from −105 to −107, −103 to −99, −97 to −94, −92 to −86 and −88 to −84 ppm, respectively.

In liquid state NMR the chemical shift depends on the structural details such as bond angle, bond length associated with a particular structure. But in solid NMR experiments the changes in chemical shifts due to above parameters are not adequately reflected in respective peaks because of higher line widths. However, special experiments can reveal the change in chemical shift if carried out with high-resolution mode. Amorphous non-zeolitic silica can often be identified at a higher shift [6]. The framework silicon to aluminum ratio of the catalyst can be calculated from the ^{29}Si MAS (magic angle spinning) NMR spectra with the fact that the number of silicon atoms in various possible environments is proportional to the MAS NMR intensity as long as the Lowenstein's rule is valid. However, in commercial FCC catalysts, presence of silica and alumina from various sources other than zeolites like matrix, binder, clay complicates the analysis by broadening and interfering with the environment of the characteristic ^{29}Si peaks. ^{29}Si CP-MAS (cross polarization with MAS) was often used to observe the existence of contributions from surface structures and defect structures ended by Si–OH groups. CP experiments have shown that hydrothermally dealuminated zeolites contain relatively large amount of Si–OH groups presumably on the internal surfaces.

The acidic properties of zeolites are intimately related to the nature and distribution of the aluminum atoms in the framework and in the cage morphology. Therefore, a careful examination of aluminum environment is necessary for understanding the catalytic properties. Usually the peaks at 60 and 0 ppms in ^{27}Al MAS NMR spectrum are ascribed to tetrahedral framework aluminum species and octahedral aluminum atoms in extra framework structure [9]. Bourgeat-Lami et al. proposed for the first time that the octahedrally coordinated framework aluminum sites could be converted to tetrahedral aluminum upon adsorption of certain molecules [10]. The presence of aluminum species that reversibly convert their symmetry upon NH_3 adsorption was also observed in zeolite HY [11]. Four and six coordinated aluminum are also observed in amorphous silica alumina materials [12]. The presence of penta-coordinated alumina has also been detected as surface defect sites at a shift value of 30 ppm. However, the aluminum associated with four types of Brönsted acid sites Si(4Al), Si(3Al), Si(2Al) and Si(1Al) in the next nearest neighbors could not be distinguished due to high quadrupolar broadening of Al (MHz range). The spectral resolution is suffered by the second order quadrupolar interaction of the central transition that could not be minimized with MAS, and this interaction not only broadens the resonances but also moves the isotropic chemical shifts in 1D MAS spectrum. MQMAS (multiple quantum MAS) NMR developed by Frydmann and Harwood [13] removes the second order quadrupolar broadening thus allowing the detection of pure isotropic spectra [14–17]. Isotropic chemical shift and quadrupolar parameters determined from the analysis of MQMAS spectra can be used to simulate the ^{27}Al MAS spectra leading to quantitative information about the aluminum species [17].

A few cases of catalyst deactivation in FCC were studied [18–21]. Deactivation of FCC catalysts not only yields a sudden drop in activity but also changes in selectivity. However, the formation and chemical nature of coke on catalysts have long been of scientific importance worldwide. The nature and composition of coke depend on nature of feeds, type of catalysts and process conditions [8,22]. In general, deactivation by coking occurs due to site coverage (active site poisoning by coke deposition) and pore blockage (active sites inaccessible to reactants). In a recent study by Occelli et al. [19] have shown that during gas oil cracking at micro activity test (MAT) conditions in FCC, coke deposits on the pore walls thus decreasing pore widths and consequently prevent molecular diffusion to the active sites. Various mechanisms for active site coverage, pore filling as well as pore blockage have been observed in FCC [23]. The influence of deactivation by coking depends very much on the nature of coke, its structure and morphology and exact location of coke deposition on catalyst surface [24]. Initially coke formation follows the adsorption of coke precursors on the catalysts surface. In general 'conjunct polymerization' (the combination of simultaneous polymerization, isomerization, β-scission, cyclization and hydrogen transfer reaction is called conjunct polymerization) is a principal contributor to coke formation in acid catalyzed reactions. Under severe process conditions, cyclization of alkyl aromatics forms condensed polycyclic aromatics and these species are more important coke precursors. Alkyl aromatics with more than four carbon atoms can cyclize (self alkylate) to form alkyl indane or alkyl naphthalene. In acid catalyzed reactions ring closure involves secondary or 3° carbons in a side chain but never with a 1° one. Most acid catalysts promote the polymerization of olefins.

Solid state ^{13}C NMR has the unique ability to determine the distribution of various types of carbons such as aliphatic, aromatic and naphthenic present in the catalytic hard coke [8,25,26]. FCC coke contains only 1–2% of carbons on the spent catalysts. The high concentration of coke is necessary to achieve sufficient sensitivity for characterizing coke by solid state ^{13}C NMR which is achieved by demineralizing the aluminosilicate matrix to concentrate coke content [26]. Single hard pulse excitation (SHPE) has been considered as the best technique for quantitative ^{13}C NMR analysis of coals and solid fuels, but with a considerable sacrifice in sensitivity since long recycle times are required to ensure complete restoration of equilibrium magnetization [8]. The CP in combination with MAS is a very sensitive technique to characterize different types of carbons in short-time scale [26]. Although this technique is mostly used for detection and identification of structural moieties, it can be employed for semi quantitative analysis provided optimized contact times are used. The dipolar dephasing (DD) in combination with MAS can differentiate the aromatic carbons of having attached hydrogens or not based on the relaxation behaviour in coke. Once we identify the chemical shifts of various carbons present in coke from SHPE and CP-MAS NMR, CP dynamic studies can give various properties of these individual groups of carbons.

2. Experimental

2.1. Samples

Four catalysts, fresh, equilibrium, spent and regenerated, were collected from the FCC unit of an Indian refinery. All these catalysts were dried at 60 °C for overnight to remove the surface adsorbed species, if any present. These catalysts are termed as cat1, cat2, cat3 and cat4, respectively.

2.2. NMR experiments

All the NMR experiments were carried out on a Bruker DRX-300 Avance spectrometer with a Bruker's dual 4 mm MAS probe. Approximately 150 mg of finely powered sample was packed in 4 mm zirconia rotor for each experiment. The rotor was spun at 10–12 kHz speed. The ^{29}Si SHPE-MAS spectra were taken by using $\pi/2$ pulse of 4 μs and pulse interval of 10 s with 1200 number of scans for each sample. The spectra were processed with 40 Hz line broadening and chemical shifts were determined relative to tetra methyl silane as external reference. The ^{29}Si MAS spectra were deconvoluted using Bruker WINFIT simulation programme to obtain quantitative data. The ^{29}Si CP-MAS experiments were carried out under Hartmann-Hahn condition using contact time 5 ms and recycle delay of 1 s. The $\pi/2$ pulses used for ^{1}H and ^{29}Si were 2 μs and 4 μs, respectively. Two thousand scans were accumulated to obtain significant signal to noise ratio for each experiment.

All ^{27}Al MAS NMR experiments were carried out with $\pi/20$ pulse and a 1 s recycle delay to accumulate 1200 scan for each sample. The samples were spun at 12 kHz spinning rate. ^{27}Al MQMAS spectra were obtained using a z-filter method [16] where

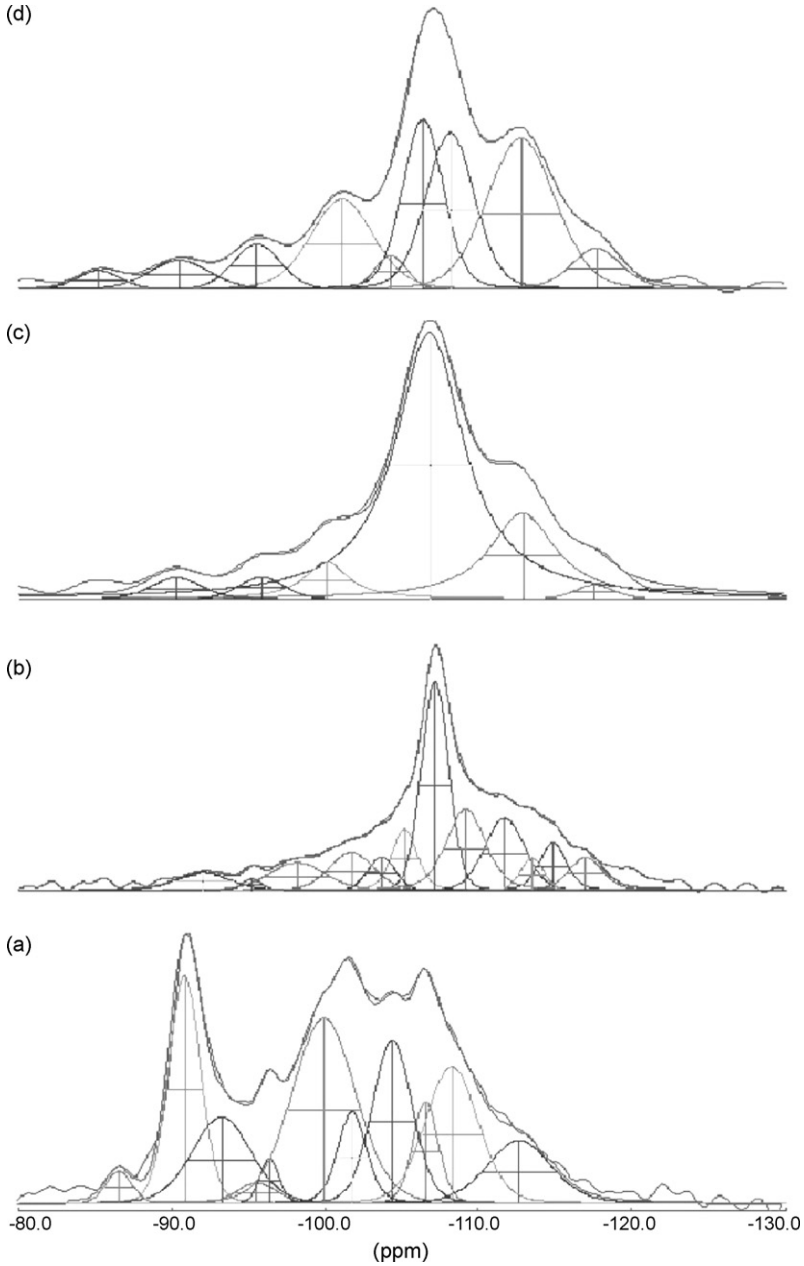

Fig. 1. ^{29}Si MAS NMR spectra of cat1 (a), cat2 (b), cat3 (c) and cat4 (d). Upper traces are the spectra and below peaks are deconvoluted profiles of individual Si sites of respective catalysts.

Table 1
Local individual Si peak intensity and width of different Si(*n*Al) sites obtained from deconvolution of ^{29}Si MAS NMR of four catalysts

Si sites	cat1		cat2		cat3		cat4	
	$\nu\Delta_{1/2}$ (Hz)	I (%)	$\nu\Delta_{1/2}$ (Hz)	I (%)	$\nu\Delta_{1/2}$ (Hz)	I (%)	$\nu\Delta_{1/2}$ (Hz)	I (%)
Si(4Al)	119	1.6	–	–	–	–	–	–
Si(3Al)	144.9	14.4	242.1	4.4	272.5	4.5	230.9	4.2
Si(2Al)	181	1.6	89.4	10.1	212.9	5.4	236.7	6.1
Si(1Al)	289.8	23.5	203.9	7.5	285.0	14.9	279.0	12.0
Si(0Al)	181.8	13.1	115.7	17.5	186.6	18.4	196.2	19.5

the phase cycling was designed to select the coherence pathway of $0 \rightarrow \pm 3 \rightarrow 0 \rightarrow -1$ in concert with TPPI mode. The first hard pulse was to create the triple quantum coherence, while the second one was to convert the triple quantum to zero quantum coherence. RF amplitude of 103.3 and 43.61 kHz were used for the first and second pulses and their pulse lengths were optimized to be 4.4 μs and 1.85 μs, respectively. In the experiment for the third pulse low RF amplitude of 9.2 kHz was used to select the central transition. For each t_1 increment, 128 scans were used to accumulate the signal with relaxation delay of 2 s. A shearing transformation was performed after 2D Fourier transformation. The chemical shift was referenced to $[Al(H_2O)_6]^{3+}$. From the 2D contour, isotropic induced shifts were calculated for each Al sites. 'Bruker WINFIT' programme using the value of quadrupolar parameters obtained from 3QMAS Al experiments as base value the ^{27}Al MAS spectra are simulated.

2.3. Surface area

Nitrogen sorption isotherm at liquid nitrogen temperature was obtained with Micrometrics ASAP 2010 unit using a volumetric technique. Prior to analysis, samples were out-gassed in vacuum at 400 °C for at least 8 h. A precise description of the micropore system was obtained by sending successive increments of analysis gas and waiting for thermal equilibration. BET surface areas were calculated from nitrogen uptakes at relative pressures ranging from 0.05 to 0.30.

2.4. X-ray diffraction

Powder XRD patterns were obtained on a Siemen's X-ray diffractometer using Cu K_α radiation for all catalysts. All the catalysts are dried at 60 °C to remove the surface adsorbed species prior to loading. The scan speed was 5°/min and the scan range was 5–50°. The unit cell size was determined by using NaY zeolite as reference material. The strong reflections were observed in the region $15^\circ < 2\theta < 56^\circ$.

3. Results and discussion

3.1. Local Si structures

Since NMR has the unique ability to probe the local structures, ^{29}Si MAS NMR of all the four catalysts have shown the variations in the silicon environments at the first coordination (Q^4) sites as shown in Fig. 1. Isotropic chemical shift values are directly obtained from the spectra, however, due to the strong dipolar broadening along with the severe chemical shift dispersivity peaks for individual five Q^4 sites (Si(*n*Al)) are overlapped masking the detailed information. They do have the structural variations, which are being qualified and quantified after doing the proper deconvolution. During the deconvolution, all the Si sites of Y zeolites, defect Si sites, clay and amorphous silica are being considered but kaolin, additive and amorphous silica are not considered for our discussion since we are only focused for the changes in zeolitic (Y) component of catalyst. The spectral profiles of all the catalysts are very different (Fig. 1). In the deconvoluted spectra, signals approximately at −86.5, −91.5, −95.5, −99.9 and −104.4 ppm are the characteristic peaks for Si(4Al), Si(3Al), Si(2Al), Si(1Al) and Si(0Al) sites, respectively. However, isotropic chemical shift values vary slightly from cat1 to cat4 depending on their local structural changes. Peaks at −112, −106 and −115 ppm are used for total simulation of the Si NMR spectra, these peaks are the indicative of siliceous ZSM-5 peaks used as additive in these commercial FCC catalysts. Similarly resonance at −93.2 ppm and upfield peak at −110.0 ppm arise due to kaolin and amorphous extra framework silica (defect) though used for the reconstruction of whole Si spectra, are not used in discussion. Henceforth, for our discussion we are considering only the five Si peaks of Y zeolites to find out the local structural changes taking place from fresh to regenerate stages in the cracking unit. All the NMR parameters for these five peaks obtained from the deconvolution are given in Table 1. The normalized relative intensities (I) given in the table are directly proportional to their relative population of the respective sites whereas the peak width at half height ($\Delta_{1/2}$ in Hz) says about the local environmental changes at the respective sites due to electronic environment (bonding, electron distribution, etc.), anisotropic effect (chemical shift and dipolar effect) and local symmetry (quadrupolar effect).

A close look at Table 1 envisages that only the fresh catalyst has all the five Si sites but Si(4Al) sites are not detected in rest three catalysts. Thus, there is a greater magnitude of depletion of these

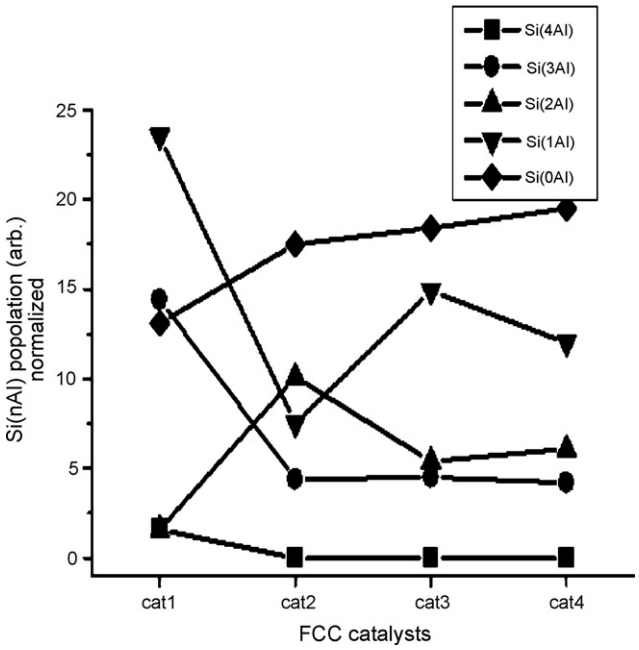

Fig. 2. Population (intensity) change profiles of five Si(*n*Al) sites of first coordination sphere from cat1 to cat4.

sites once the fresh catalyst is made to e-cat. This is due to the fact that during the equilibrium catalyst (e-cat) preparation from fresh catalyst, dealumination depletes this Si(4Al) sites abundantly because of the four Al atoms present at this site which makes it easier to be dealuminated. The relative changes in their site populations from the fresh to regeneration stages i.e. from cat1 to cat4, are very interesting as shown in Fig. 2. During equilibration, Al atoms of Si(3Al) and Si(1Al) migrate to extraframework with simultaneous increase in population of Si(2Al) units. There is also increase in population of Si(0Al) units but with lesser degree as

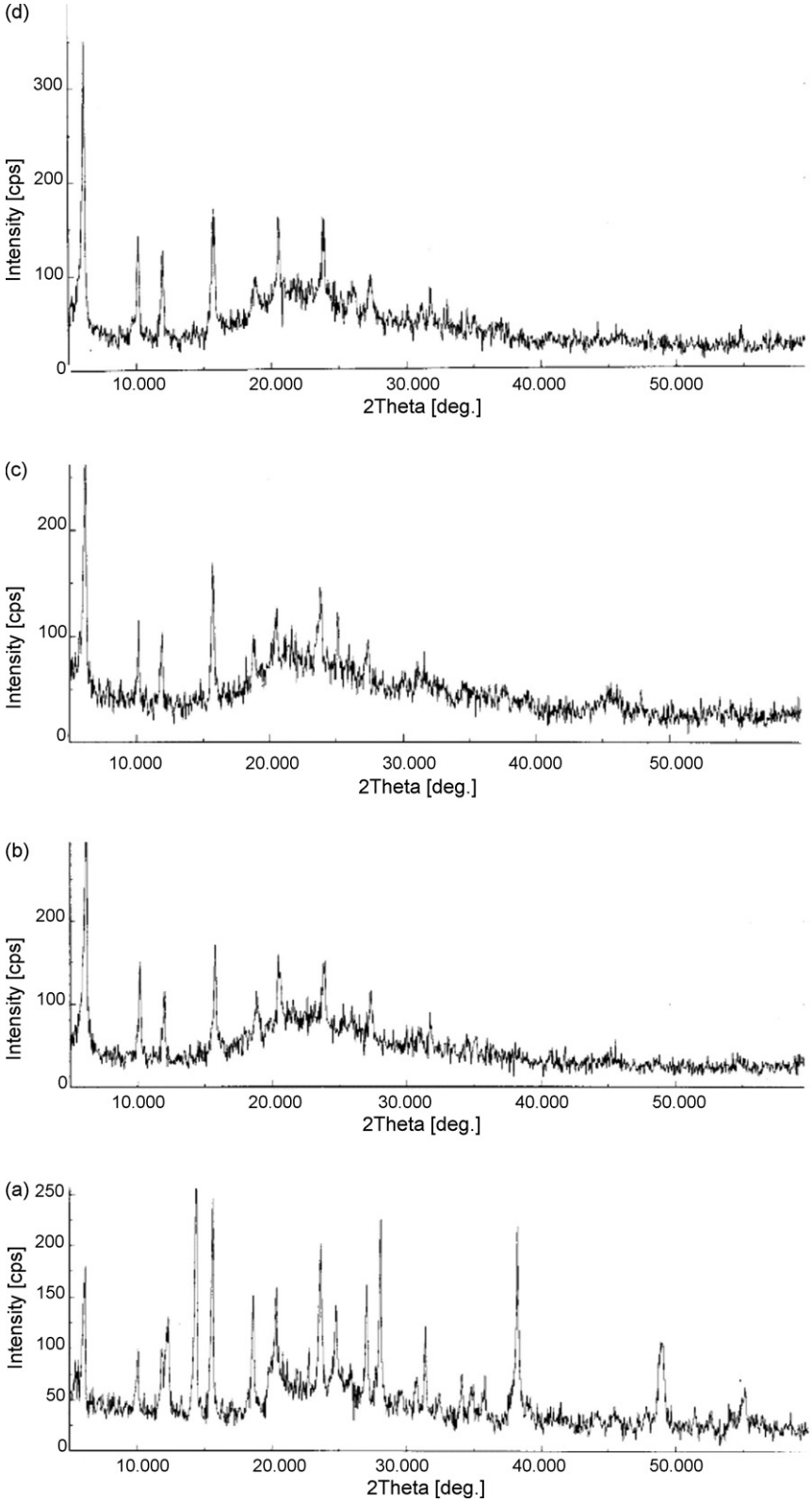

Fig. 3. XRD patterns of cat1 (a), cat2 (b), cat3 (c) and cat4 (d) showing the loss of crystallinity.

compared to Si(2Al) units (smaller slope in Fig. 2). Under cracking condition, Si(3Al) sites remains almost unaffected, population of Si(1Al) increase at the expense of Si(2Al) and there is negligible change in the population of Si(0Al). During regeneration process, population of Si(1Al) sites depletes, increase in population of Si(2Al) at the expenses of Si(3Al). There is gradual increase in Si(0Al) population from fresh to regeneration conditions due to continual dealumination process. Relative distribution of Si(*n*Al) sites are found to be quite similar in cat3 and cat4. From the line width analysis it is found that with decrease in neighboring Al atoms in contrast line width increases with removal of quadrupolar atoms. This envisages that the chemical shift anisotropy through Si–O–Al dominates over the quadrupolar interaction and plays a vital role in governing the electronic environment about Q^4 Si sites. Here, other factors considered for line broadening are the distribution of Si–O–Al bond angles and bond distances and Si–Al dipolar interactions.

3.2. Effect on Si/Al ratio, unit cell size and microcrystallinity

NMR provides most reliable and direct determination of framework Si/Al ratio. When Si/Al ratio was calculated from the ^{29}Si NMR data, it revealed that there is increase in Si/Al ratio. Increase in the ratio envisages that there must be migration of Al atoms from the framework structure thereby creating the vacancies. In order to fill these vacated Al lattice sites, Si atoms migrate from one site to other to rearrange the lattice structure from fresh catalyst to regenerated one. XRD patterns show that there is progressively loss in crystallinity from fresh to regenerated catalysts as shown in (a)–(d) in Fig. 3. Changes in Si/Al ratio calculated from NMR and XRD are shown in Fig. 4(a) along with the change in unit cell size (UCS) calculated from XRD. $(Si/Al)_{NMR}$ increases up to spent catalyst and then decreases whereas, $(Si/Al)_{XRD}$ increases almost linearly up to spent catalyst after that it increases slowly in contrast to NMR finding. This is because the calculation by XRD is considered for long range ordering along with the total lattice, whereas, by NMR only local effect with only the framework is in effect neglecting the contribution from extra-framework structure. Thus, from spent to regeneration stage, migration of framework Si atoms to amorphous structure contributes for decrease in Si/Al. This is in agreement with the decrease in UCS as shown in Fig. 4 where depletion of Si units from framework structure imposes the shrinkage in unit cell. XRD patterns also show the decline of the crystallinity from cat1 to cat4. When plotted the percentage of crystallinity with respect to cat1, it is found that crystallinity nonlinearly decreases up to 50% as shown in Fig. 4(b). The plot of surface area by BET method in Fig. 4(b) shows a linear decrease up to spent catalyst after that it shoots up. Initial reduction in area from fresh to e-cat is due to proportionate mixing of regenerate catalyst with fresh catalyst where regenerated catalyst has relatively less surface area compared to fresh one. During cracking further reduction in area in spent catalyst is due to deactivation of catalytic sites by coking. By regeneration process, since some cokes are burnt, hence there is increase in area due to removal of cokes from pores/surfaces.

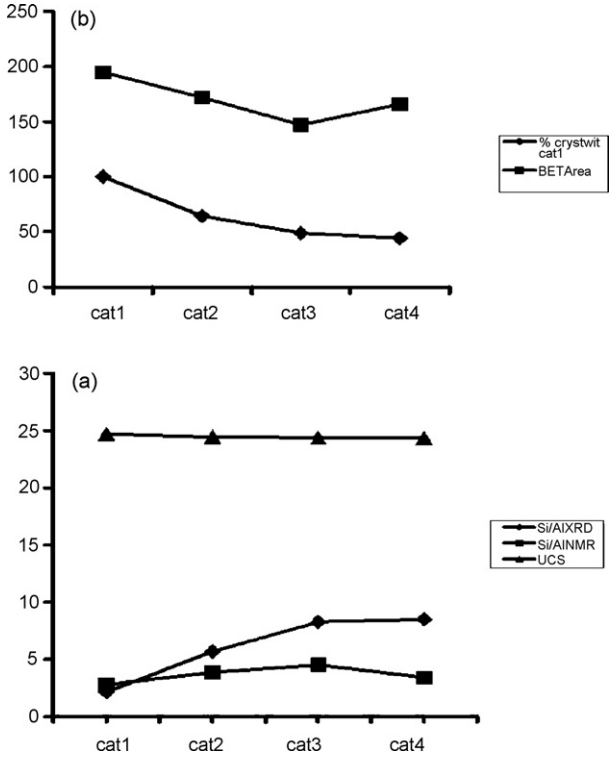

Fig. 4. Plots showing the changes in (a) Si/Al ratios from NMR and XRD and unit cell size from cat1 to cat4 and (b) % of crystallinity with respect to cat1 and BET surface area.

3.3. Changes in Al structures

^{27}Al MAS NMR can provide both qualitative and quantitative information of various Al species present in framework and extraframework structures. Fig. 5 shows the 1D ^{27}Al MAS NMR of all four catalysts. However, simulation of these spectra is essential to differentiate the Al species existing in both octahedral (O_h) and tetrahedral (T_d) geometries and thereby to extract the information. Since the approximate values of quadrupolar coupling constants (C_Q) are essential for simulation of these spectra, we have performed the ^{27}Al 3QMAS NMR of cat1 to get the different inequivalent T_d and O_h sites and their C_Q values. Analysis of the 3QMAS NMR gives two each chemical shift values of T_d and O_h sites with their induced chemical shift values and second order quadrupolar coupling values as shown in Table 2 (spectra is not shown). These values are used in 1D MAS NMR spectral simulation by using WINFIT software from Bruker and simulated spectra are shown along with the 1D spectra in Fig. 5. A close look on the simulated spectra shows the different line shapes for various Al sites and is not like isotropic peaks. This indicates some Al sites are having the chemical shift anisotropies and further broadened by quadrupolar effects. Various parameters obtained from simulation are given in Table 3. Table data exhibits four types of Al species, two for octahedral and two for tetrahedral symmetries. As the FCC catalysts is a complex mixture of zeolites and matrix, not only the zeolitic Al sites but also the Al sites from matrix are being detected by Al NMR. The T_d and O_h aluminum sites having the low field shifts with high coupling constant values are assumed to come from the matrix whereas, high field shifts with lower SOQE values are from zeolitic part of the catalyst. It is observed that the second order quadrupolar coupling constant of tetrahedral sites are comparatively higher than the octahedral sites. This may be due to imposition of more asymmetry at the acidic sites of Al atoms owing to stronger electric field gradients. In these cases η_Q values are

Table 2
Chemical shifts, isotropic chemical shifts, induced chemical shifts and second order quadrupolar coupling values of tetrahedral and octahedral aluminum sites of cat1 obtained from 3QMAS NMR

	δ_1 (ppm)	δ_2 (ppm)	δ_{isoCS} (ppm)	δ_{IS} (ppm)	SOQC (MHz)
O_h	16.0	4.0	7.8	2.7	3.87
T_d	66.0	59.0	63.4	3.0	4.484

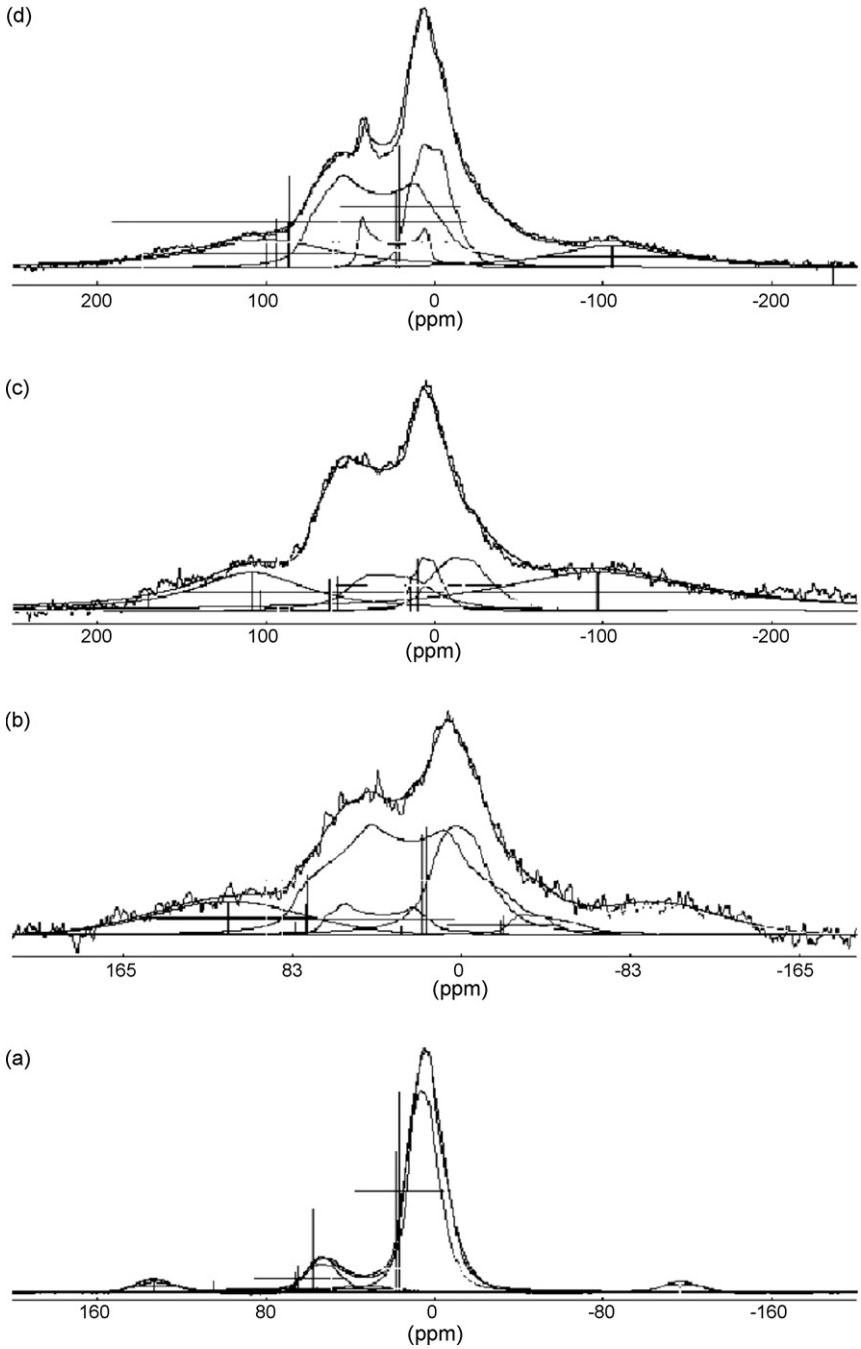

Fig. 5. ^{27}Al 1D MAS NMR spectra of cat1 (a), cat2 (b), cat3 (c) and cat4 (d). Upper traces are the experimental spectral profiles while peaks at below are the simulated peaks for each Al sites.

comparatively low indicate the lower symmetry. More quadrupolar coupling constant values for cat3 and cat4 extensively broaden the spectral width due to severe structural changes as a result of high temperature effects as well as coking at sites. Presence of less intense peak around 40 ppm indicates the formation of distorted tetrahedral aluminum species in both spent and regenerated catalysts resulting from partial destruction of framework. This also confirmed from resulted decrease in microcrystallinity from X-ray data. Since the population of both O_h and T_d sites are not conserved, interconversion of these sites is favoured within the framework structure. This is supported by the fact that the octahedrally coordinated framework Al sites in HY and ZSM-5 [10] and in non-hydrated Y zeolites [15,27] are detected. Besides the usual O_h and T_d interconversion between framework and extraframework/matrix, there is also possibility of conversion well within the extraframework/matrix. This is because of presence of 0 ppm peak due to flexible octahedral Al in matrix [8].

3.4. Nature of coke

In earlier section, we have discussed that the Si(2Al) and Si(3Al) sites deplete by participating in cracking, these sites along with Si(3Al) are deactivated fast by coking. So we want to understand the nature and structure of coke formed at these sites that can help to understand the deactivation mechanism. Since we did not get soft coke while extracting coke from both regenerated and spent

Table 3
Chemical shifts, asymmetry parameter, quadrupolar coupling constant and second order quadrupolar coupling values of tetrahedral and octahedral aluminum species obtained from ^{27}Al 1D MAS spectral simulation of four catalysts

	cat1				cat2			
	O_h		T_d		O_h		T_d	
δ_{cs} (ppm)	8.5	16.8	56	64	6.8	16.9	76.6	87.9
η_Q	0.11	0.54	0.49	0.44	0.22	0.22	0.22	0.45
C_Q (MHz)	3.4	3.26	4.66	3.33	4.8	4.1	6.12	7.66
SOQC (MHz)	3.4	4.21	4.83	3.43	4.83	4.13	6.16	7.91
	cat3				cat4			
	O_h		T_d		O_h		T_d	
δ_{cs} (ppm)	10.3	16.4	57.3	65.7	7.6	20.5	56	86.4
η_Q	0.5	0.48	0.2	0.5	0.6	0.48	0.04	0.3
C_Q (MHz)	4.99	3.45	5.67	7.5	5.5	4.25	5.82	7.33
SOQC (MHz)	5.15	3.58	5.71	7.8	5.82	4.41	5.83	7.44

catalysts, therefore, soft cokes are almost converted to insoluble cokes. No substantial amount of hard coke was found from regenerated catalyst. This may be due to treatment of spent catalyst with air and steam at elevated temperature in the regeneration unit, thus burning most of the coke present in spent catalyst. Therefore, the structure of coke derived here is extracted from spent catalyst. Both ^{13}C SHPE-MAS and CP-MAS spectra are shown in Fig. 6. Though SHPE-MAS NMR is used for quantitative analysis of carbon type structures, CP-MAS helps to identify various types of carbons present in coke due to enhancement of sensitivity and thus augments to estimating structural parameters by SHPE-MAS NMR. From CP-MAS spectra (Fig. 6(b)), it is observed that (i) a poorly defined small hump at 10–50 ppm indicates very small quantity of aliphatic compounds/groups are present, (ii) an intense and broad peak at 130 ppm says about the presence of both protonated and non-protonated aromatic carbons in coke with relatively high quantity, (iii) presence of heteroatomic aliphatic carbon (C_{ali}–O–) indicated by the presence of a strong peaks within 50–90 ppm region and (iv) a peak at −105 ppm indicates the presence of pyrollic carbons. Both the above (iii) and (iv) observation are supported by elemental analysis which gives the presence of oxygen in coke extract. Various structural parameters derived from ^{13}C SHPE/CP-MAS, CP-DD and CP Dynamic NMR are given in Table 4.

Table 4
Various structural parameters of coke obtained by different ^{13}C solid state NMR

Structural parameter	Value		
SHPE and CP-MAS NMR			
f_a	0.96 (SHPE)		0.41 (CP)
f_a^{NP}		0.67	
f_a^{P}		0.28	
γ_{ar}		1.96	
N_{peri}		13.0	
f_{ali}^{CHO-}		1.0	
^{13}C CP-DD NMR			
T_{2G} (μs)		2.7	
T_{2L} (μs)		208	
I_{2G} (normalized to 1)		0.30	
I_{2L} (normalized to 1)		0.70	

Structural parameter	δ (ppm)	T_{CH} (μs)	$T_{1\rho}$ (H) (ms)
^{13}C CP dynamics			
Aromatic carbons including protonated and bridgehead	126.1	74	2.4
Aromatic/olefinic carbons attached to pyrollic group	105.4	49	13
	88.9	30	14
Aliphatic carbons attached to etherial groups	71.5	328	14
	64.8	142	12
Aliphatic carbon	20.8	98	1.5

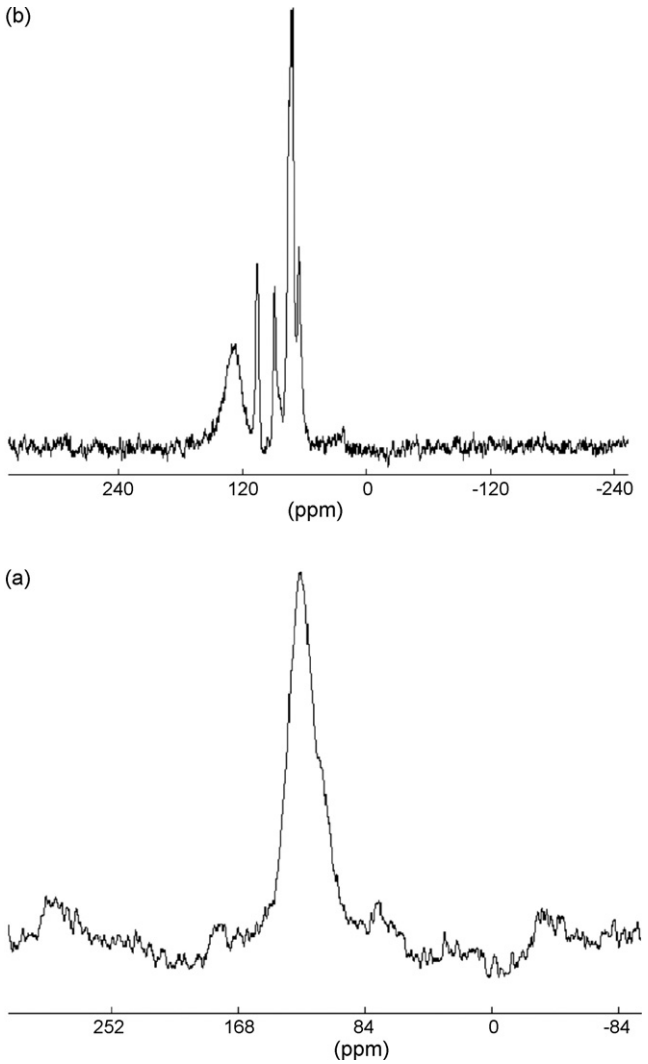

Fig. 6. ^{13}C SHPE-MAS NMR spectra (a) and ^{13}C CP-MAS NMR spectra (b) of hard coke extracted from spent FCC catalyst.

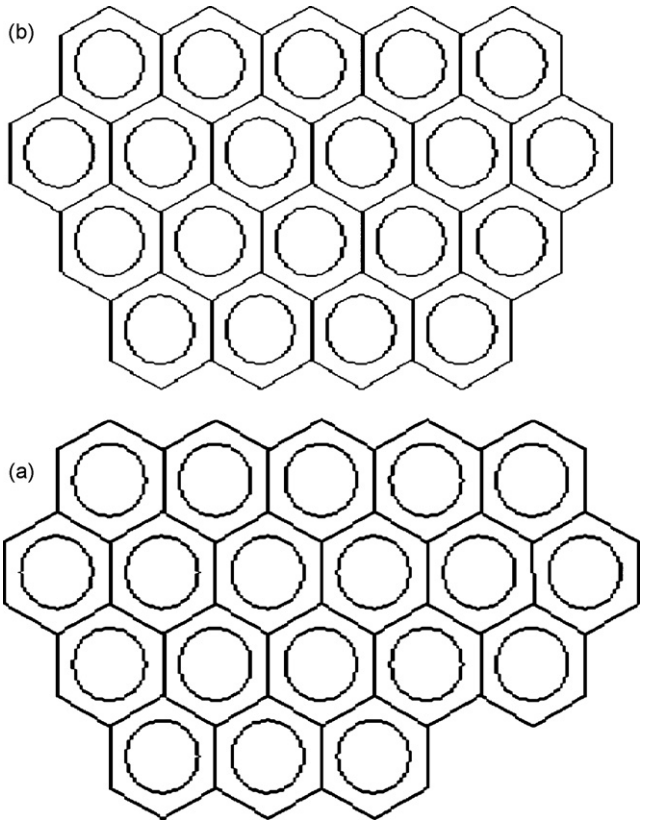

Fig. 7. Most probable condensed aromatic structures modeled from NMR data of coke. For (a) condensation index (γ) = 1.89, no. of pericondensed aromatic rings (NPAR) = 12 and no. of catacondensed aromatic rings (NCAR) = 7 and for (b) condensation index (γ) = 2.0, no. of pericondensed aromatic rings (NPAR) = 13 and no. of catacondensed aromatic rings (NCAR) = 7.

The coke is found to be highly aromatic having aromaticity (f_a) of 0.96 as deduced from SHPE NMR data. CP NMR under represents this value of 0.41, as polarization transfer technique used here does not quantify the carbons properly. Out of the aromatic carbons, around 67% is non-protonated carbons that represent more condensation of aromatic rings in coke. This observation is further supported from CP-DD NMR data (Table 4) where non-protonated aromatic carbons have around 70% intensity as represented by I_{2L} and protonated carbon intensity is around 29% (I_{2G}). Thus these types of carbons have their representative relaxation times one in ms and other in μs scale. CP dynamic technique differentiate further the carbons based on the carbon–proton relaxation time constant (T_{CH}) which is faster in the order of μs and the proton spin diffusion time constant which is very long at the order of ms in coke as shown in Table 4. These characteristic values in terms of chemical shifts (δ), cross polarization time (T_{CH}) and proton relaxation time in rotating frame ($T_{1\rho}$(H)) for aromatic carbons including protonated and bridgehead carbons, aromatic and olefinic carbons attached to pyrollic groups, aliphatic carbons and aliphatic carbons attached to etherial groups are shown in Table 4. By using these parameters, we can differentiate the various types of carbons present in coke. Since aliphatic carbon attached to CHO– group is found to be 1%, this sort of structure is assumed to be formed during either oxidation of coke at very high temperature or due to presence of oxy-functional groups present in feed. From the bridgehead carbons ($f_a^{BR} = C_{BR}/C_{ar}$), the degree of condensation (γ) is calculated as the ratio of fraction of bridgehead to peripheral aromatic carbons and is found to be 1.96. Number of pericondensed rings per average molecule (N_{peri}) is found to be 13 to fit this γ value. We modeled the average structure of aromatic coke to fit both obtained γ and N_{peri} values and found that most probable condensed ring structure of coke is as shown in Fig. 7(b) with 13 number of pericondensed aromatic rings and 7 number of catacondensed aromatic rings. It is postulated that these type of coke structures may be present either in the super-cage or at the defect surface sites (pore opening) of Y zeolites of deactivated FCC catalysts.

4. Conclusion

Various solid state NMR methods have demonstrated as a very powerful technique for molecular level characterization of industrial FCC catalysts at different stages in the cracker unit. Both Si(3Al) and Si(1Al) sites of Y zeolites in FCC catalyst decayed more under hydrothermal conditions. Cracking occurs at more probable Si(2Al) sites which are further generated from Si(3Al) sites due to dealumination. We conclude from our study that since e-cat contains relatively less Brönsted sites compared to Lewis, later sites play equally important role in the formation of carbenium ions. Crystalline structure and unit cell size decrease rapidly in spent and regenerated catalysts. Both tetrahedral and octahedral aluminum sites participate in cracking process. Symmetry around tetrahedral aluminum sites is distorted due to cracking and coking at these sites resulting higher quadrupolar coupling constant. Regenerated catalyst contains substantially very less coke compared to spent, and over all coke content is small. The coke is mostly hard coke, more condensed polyaromatic in nature and contains 13 aromatic rings at periphery.

Acknowledgements

Ms. Babita Behera would like to acknowledge CSIR, India for the grant of research fellowship. Director, IIP is thankfully acknowledged for permitting this work to be published. We also thank IIP and CSIR for funding the project OLP-521219 to partially carry out this work.

References

[1] P.B. Venuto, E.T. Habib, Fluid Catalytic Cracking with Zeolite Catalysts, Marcel Dekker, New York, 1979.
[2] M.L. Occelli (Ed.), Fluid Catalytic Cracking; Role in Modern Refining, ACS Symposium Series 375, ACS, Washington, 1988.
[3] M.L. Occelli, P.O. Conner (Eds.), Fluid Catalytic Cracking III; Materials and Processes, ACS Symposium Series 571, ACS, Washington, 1994.
[4] M.L. Occelli, P.O. Conner (Eds.), Fluid Catalytic Cracking, Marcel Dekker, New York, 1998.
[5] Indian Petroleum and Natural Gas Statistics, Ministry of Petroleum and Natural Gas Economics and Statistical Division, Government of India, New Delhi, 2004–2005.
[6] G. Engelhardt, D. Michel, High Resolution Solid state NMR for Silicates and Zeolites, Wiley, England, 1987.
[7] A.T. Bell, A. Pines (Eds.), NMR Techniques in Catalysis, Marcel Dekker, New York, 1994.
[8] B. Behera, S.S. Ray, I.D. Singh, in: Fluid Catalytic Cracking. VII: Materials, Methods and Process Innovation, Chapter 12, Elsevier, 2007.
[9] C.A. Fyfe, G.C. Gobbi, J. Klinowskii, J.M. Thomas, S. Ramdas, Nature 296 (1982) 530.
[10] E. Bourgeat-Lami, P. Massiani, F. Renzo, P. Espiau, F. Faujula, T.D. Coariers, Appl. Catal. 72 (1991) 139.
[11] B.H. Wouters, T.H. Chen, P.J. Grobet, J. Am. Chem. Soc. 120 (1998) 11419.
[12] C. Doremiux-Morin, C. Martin, J.M. Bregeault, J. Fraissard, Appl. Catal. 77 (1991) 149.
[13] L. Frydmann, J.S. Harwood, J. Am. Chem. Soc. 117 (1995) 5367.
[14] S. Ganapathy, T.K. Das, R. Vetrivel, S.S. Ray, T. Sen, S. Sivasanker, L. Delevoye, C. Fernandez, J.P. Amoureux, J. Am. Chem. Soc. 120 (1998) 4752.
[15] J.S. Van Bokhoven, A.L. Roest, D.C. Koningsberger, J.T. Miller, G.H. Nachtegaal, A.P.M. Kentgens, J. Phys. Chem. B 104 (2000) 6743.
[16] J. Jiao, J. Kanellopoulos, W. Wang, S.S. Ray, H. Foerster, D. Freude, M. Hunger, Phys. Chem. Chem. Phys. 7 (2005) 3221.
[17] J. Jiao, J. Kanellopoulos, B. Behera, W. Wang, H. Huang, V.R.R. Marthala, S.S. Ray, H. Foerster, D. Freude, M. Hunger, J. Phys. Chem. B 110 (2006) 13812.

[18] M.L. Occelli, H. Eckert, A. Wolker, M. Kalwei, A. Aurox, S.A.C. Gould, J. Catal. 196 (2000) 134.
[19] M.L. Occelli, J.P. Olivier, A. Aurox, J. Catal. 209 (2002) 385.
[20] M.L. Occelli, J. Olivier, A. Petre, A. Aurox, J. Phys. Chem. B 107 (2003) 4128.
[21] M.L. Occelli, U. Voigt, H. Eckert, Appl. Catal. A 259 (2004) 245.
[22] B. Behera, S.S. Ray, I.D. Singh, Am. Chem. Soc., Div. Petro. Chem. 51 (2006) 452 (Preprint).
[23] R.G. Menon, J. Mol. Catal. 59 (1990) 207.
[24] P.O. Connor, A.C. Powels, Studies in surface science catalysis, in: B. Delmon, G.F. Froment (Eds.), Catalyst Deactivation, vol. 88, Elsevier, New York, 1994.
[25] C.E. Snape, B.J. McGhee, S.C. Martin, J.M. Anderson, Catal. Today 37 (1997) 285.
[26] S.K. Sahoo, Siddharth S. Ray, I.D. Singh, Appl. Catal. A 278 (2004) 83.
[27] J. Jiao, S.S. Ray, W. Wang, J. Weitkamp, M. Hunger, Z. Anorg, Allg. Chem. 631 (2005) 484.